JPE Journal of Photonics for Energy

RESEARCH PAPER

Enhanced photon collection in leaf-inspired luminescent solar concentrators

Hiroto Nishimura, Kohei Okada, Atsuya Suzuki, Yuta Mizuno, and Ichiro Fujieda*
Ritsumeikan University, Kusatsu, Japan

ABSTRACT. A leaf-like structure is formed by placing luminescent plates in the vicinity of a luminescent fiber with their side surfaces facing the fiber. Its optical efficiency is expressed in terms of collection efficiency and absorptance of each luminescent component. This model allows one to calculate its optical efficiency under an arbitrary incident spectral photon flux. A clear lightguide can connect multiple fibers to transfer the photons generated by each leaf-like structure to a single photovoltaic cell. Thus, one can divide the incident area of a luminescent solar concentrator (LSC) into small regions without sacrificing its geometric gain. Lateral size reduction enhances its optical efficiency by alleviating the losses during the photon collection process. Other techniques reported for the conventional planar LSCs, such as edge mirrors and tandem structures, can be combined for further enhancement. In experiments, off-the-shelf luminescent components (2.0 mm-thick plates and 1.5 mm-diameter fibers) were used to assemble samples with various shapes. For example, the efficiency of collecting photons generated in the plates of a square device increased from 0.0052 to 0.024 by decreasing its side length from 50 to 10 mm and attaching mirrors on their outer edges. In contrast, optical efficiency is weakly dependent on leaf geometry, increasing design freedom on leaf shapes. The use of advanced luminescent materials as well as optimizing the leaf-like structure design would increase its optical efficiency further.

Keywords: photoluminescence; optical efficiency; collection efficiency; geometric gain; self-absorption

Paper 24015G received Mar. 13, 2024; revised May 22, 2024; accepted Jul. 8, 2024; published Jul. 19, 2024.

1 Introduction

A luminescent solar concentrator (LSC) was invented in the 1970s.[1] Initially, it aimed to reduce the cost of harvesting solar power by attaching small PV cells to the edge surfaces of a planar waveguide containing luminescent materials. Incident photons are converted to photoluminescence (PL) photons inside the waveguide. As they propagate toward the PV cells by repeating total internal reflection, they become concentrated. Unlike a concentrator based on mirrors and lenses, an LSC can harvest diffuse light. As the cost of PV cells continues to fall and making a large-scale device with decent efficiency remains challenging, interests in the LSC community have shifted from gigawatt power generation to other applications.[2] For example, a building-integrated photovoltaic system incorporates LSCs in building walls and windows.[3] It takes advantage of the aesthetic features of an LSC: it is semitransparent, and it comes in various colors. Nevertheless, a large-scale LSC is required to cover building walls. In a larger LSC, more

*Address all correspondence to Ichiro Fujieda, fujieda@se.ritsumei.ac.jp

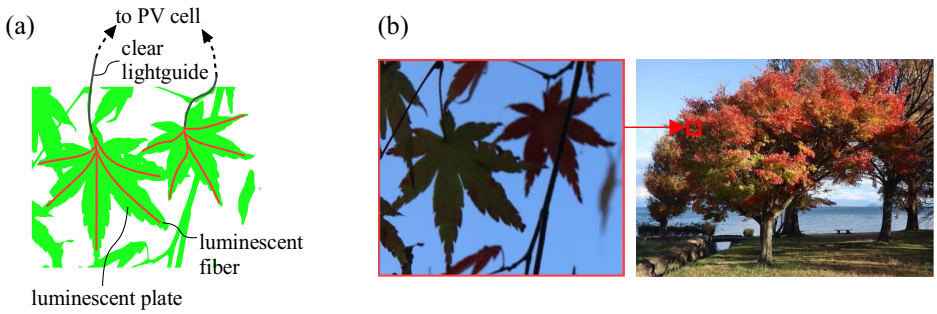

Fig. 1 The concept of energy-harvesting by volume: (a) schematic drawing of leaf LSC and (b) tree-like implementation of leaf LSCs.

PL photons are absorbed by the luminescent materials by themselves during the waveguiding process. This problem of self-absorption has been recognized since the early days.[4] Despite the efforts to develop ideal materials with a minimum overlap between absorption and emission spectra, it remains to be solved.[5,6]

This scale-up problem can be solved by connecting small-area LSCs optically. This is the idea behind the concept of "leaf LSC."[7] Luminescent plates are placed in the vicinity of a luminescent fiber with their side surfaces facing the fiber. The plates convert incident photons to first PL photons. Those entering the fiber generate second PL photons. Some of them are transported to its tip where a PV cell is attached. This is reminiscent of leaf veins carrying water and nutrients. A clear lightguide can carry the PL photons from multiple fibers to a single PV cell as shown in Fig. 1(a). Arc-bend couplers transfer photons from one lightguide to another with efficiency higher than 90%.[8] Thus, connecting N devices results in roughly N-fold increase in the incident area. To put it differently, a large-area LSC is divided into smaller regions that collect PL photons more efficiently. Lateral size reduction alleviates the photon losses caused by self-absorption and scattering in a luminescent plate. In addition, the probability of trapping PL photons is higher in a smaller waveguide because those emitted within the so-called escape cone are more likely to be transported to the PV cell. Our preliminary experiment has shown that the optical efficiency of a square leaf LSC decreases with its side length.[9] Furthermore, as shown in Fig. 1(b), leaves in a tree have various colors and they overlap with each other. Incoming photons unabsorbed and/or scattered by one leaf can be absorbed by other leaves. One can utilize the area for installing solar panels efficiently by this scheme of "energy-harvesting by volume." In addition, a modular design provides flexibility. For example, high yield is expected by manufacturing small modules. Those damaged during operation can be replaced by new ones. When new luminescent materials are developed, they can be incorporated in the leaf modules to boost the system performance.

Further studies are needed to reveal the potential of this concept. While its scalability is an advantage, it is still desired to enhance photon collection in a single leaf module. In this respect, various techniques have been reported for conventional planar LSCs. In addition to lateral size reduction, placing a reflector beneath its waveguide and a tandem structure enhance their characteristics.[10] These designs can be adopted to improve the optical efficiency of a leaf LSC. The effect of leaf shapes is also of interest.

In this paper, we express the optical efficiency of a leaf LSC in Sec. 2. Section 3 describes single-spot excitation technique for characterizing its photon collection process. With position-dependent collection efficiency at hand, one can analytically calculate its optical efficiency for an incident photon flux with an arbitrary spectrum and an arbitrary intensity distribution. In Sec. 4, a white light source is used to excite a leaf LSC uniformly for quickly measuring its average optical efficiency. We show how some familiar designs enhance photon collection in leaf LSCs.

2 Performance Metrics

It has been recommended to report power conversion efficiency (PCE) for specifying the performance of an LSC.[11] It is defined as the ratio of the output electric power to the optical power

incident on its surface. Nevertheless, it depends on the properties of specific PV cells used by the LSC as well as the spectral irradiance at its incident surface. For designing and/or evaluating an optical system, it is desirable to separate PV characteristics from PCE. Because irradiation condition varies in a real-world application, a model that can handle an arbitrary incident spectral photon flux is useful. In this section, we first review the performance metrics of an LSC and then express the optical efficiency of a leaf LSC.

2.1 Metrics for LSCs

Because an optical concentrator system concentrates an incident photon flux, the ratio of photon fluxes at its incident surface to those at its exiting surface is a relevant metric. Let us call it optical concentration factor C_{opt}. It is expressed as

$$C_{\mathrm{opt}} = G_{\mathrm{geo}}\eta_{\mathrm{opt}}, \tag{1}$$

where G_{geo} is the geometric gain (the areal ratio of the two surfaces) and η_{opt} is the optical efficiency (the probability of an incident photon resulting in a photon at the exiting surface). If the quantum efficiency of a PV cell were independent of wavelength within the range of interest, adding concentrator optics would increase the photocurrent by this factor.

In an LSC, incident photons are absorbed, and PL photons are collected by its PV cell. Hence, one can express the term η_{opt} in Eq. (1) as follows:[5]

$$\eta_{\mathrm{opt}} = \eta_{\mathrm{abs}}\eta_{\mathrm{col}}. \tag{2}$$

The term η_{abs} is the absorptance of the luminescent plate. It can be calculated by Lambert-Beer's law for a photon flux with an arbitrary spectrum $S_{\mathrm{in}}(\lambda)$ and Fresnel equations for an arbitrary incident angle. Denoting the absorption coefficient of the luminescent plate at wavelength λ as $\mu(\lambda)$, its thickness as d, and the reflectance at the surface as R, it is expressed as follows in case of normal incidence:

$$\eta_{\mathrm{abs}} = \frac{(1-R)\int(1-e^{-\mu(\lambda)d})S_{\mathrm{in}}(\lambda)\mathrm{d}\lambda}{\int S_{\mathrm{in}}(\lambda)\mathrm{d}\lambda}. \tag{3}$$

The term η_{col} in Eq. (2) is called the collection efficiency. It is defined as the probability of the absorbed incident photon resulting in a PL photon at the PV cell. Because some PL photons are lost during the collection process, η_{col} depends on the position where they are generated. For LSCs with polygonal and curved luminescent plates, one can calculate η_{col} as a function of the coordinates of the excitation spot analytically.[12] Because further study is needed to extend this analysis to a leaf LSC, we resort to experiments to determine η_{col} in Sec. 3.

2.2 Metrics for Leaf LSCs

Let us express the optical efficiency of a leaf LSC in terms of η_{abs} and η_{col}. The performance of LSCs with fiber geometry has been studied by ray tracing[13] and experiments.[14] The configuration of a leaf LSC is equivalent to such a fiber LSC and two luminescent plates with their edge surfaces facing the luminescent fiber. Thus, the photocurrent of a leaf LSC has two origins: the PL photons generated by the fiber directly and those generated by the two-stage photoconversion process. So does its concentration factor. Using Eqs. (1) and (2), it is expressed as

$$C_{\mathrm{opt}} = \frac{A_F}{A_{\mathrm{PV}}}\eta_{\mathrm{abs-F}}\eta_{\mathrm{col-F}} + \frac{A_P}{A_{\mathrm{PV}}}\eta_{\mathrm{abs-P}}\eta_{\mathrm{col-P}}, \tag{4}$$

where A_{PV} is the area of the PV cell. It is equal to the cross-sectional area of the fiber in this case. The footprints of the fiber and the plates for normally incident photons are denoted as A_F and A_P, respectively. The subscripts for the absorptance and the collection efficiency ($-F$ and $-P$) indicate the respective probabilities of each component. Noting that the geometric gain of a leaf LSC is equal to $(A_F + A_P)/A_{\mathrm{PV}}$, its optical efficiency is expressed as

$$\eta_{\mathrm{opt}} = \frac{A_F}{A_F + A_P}\eta_{\mathrm{abs-F}}\eta_{\mathrm{col-F}} + \frac{A_P}{A_F + A_P}\eta_{\mathrm{abs-P}}\eta_{\mathrm{col-P}}. \tag{5}$$

The term η_{abs-P} can be calculated by Eq. (3). One can calculate the term η_{abs-F} by varying the parameter d in Eq. (3) and averaging the results. Hence, if the terms η_{col-F} and η_{col-P} are known, η_{opt} can be calculated for an arbitrary incident spectrum.

Note that the term η_{col-P} is defined as the probability of the incident photon absorbed by the plate resulting in a PL photon at the PV cell. It can be expressed as the product of each probability associated with the series of events, namely waveguiding the PL photons in the plate, coupling them to the fiber, converting them to second PL photons, and waveguiding them to the PV cell.[7] Analysis on each step will fine-tune the leaf design in future. In the experiments described below, we assemble a leaf LSC with off-the-shelf components and measure its collective probability η_{col-P}.

3 Single-Spot Excitations

In this section, we determine position-dependent optical efficiency η_{opt} of a square leaf LSC by exciting its single spot with a laser beam. Its collection efficiency η_{col} is determined for each excitation point from Eq. (2). A similar technique was used to characterize a square device based on two-stage photoconversion with a main interest in radiation detector applications.[15]

Two strategies are adopted to enhance η_{opt} in the experiment below. One is to reduce the side length of the luminescent plates. The other is to attach mirrors to their outer edge surfaces.

3.1 Sample Preparation

The square samples shown in Fig. 2(a) were manually assembled with off-the-shelf components. The five samples on the right have mirrors on their edge surfaces. The side length of the square samples L varies from 10 to 50 mm in 10 mm steps. The plates emitting in green are 2.0 mm-thick luminescent acrylic plates (Model 1305L, Kanase Inc., Japan). Another plate from Kanase emitting in orange (Model 9989) is used for the tandem structure described in Sec. 4.2. The rods emitting in red are 1.5 mm-diameter luminescent fibers (Model FFOR-60, Plastruct, Inc.).

The samples in Fig. 2(a) are prepared as follows. Two 2.0 mm-thick luminescent plates are bridged with a 10 mm-wide reflective film (bottom mirror). A 25 μm-thick adhesive optical film with a refractive index of 1.48 (Model M3D49, Mecanusa Inc., Japan) is used to attach the plates and the reflective film. The gap between the two plates is 1.8 mm. A 1.5 mm-diameter luminescent fiber is inserted into this gap. The fiber just sits on the adhesive film backed by the bottom mirror. It is not completely straight. For these reasons, there are some regions of the fiber in contact with the plates and the adhesive film. The fiber has a 5 mm-long protruded section for easy handling in the experiment at the expense of the PL photon losses by this extra distance. The same adhesive optical films are used for attaching the reflective film to the edge surfaces of the plates.

As shown in Fig. 2(b), the edge surfaces of the plates appear flat and clear. They are polished by a supplier. The picture also shows that there are some structures inside the fiber and that some

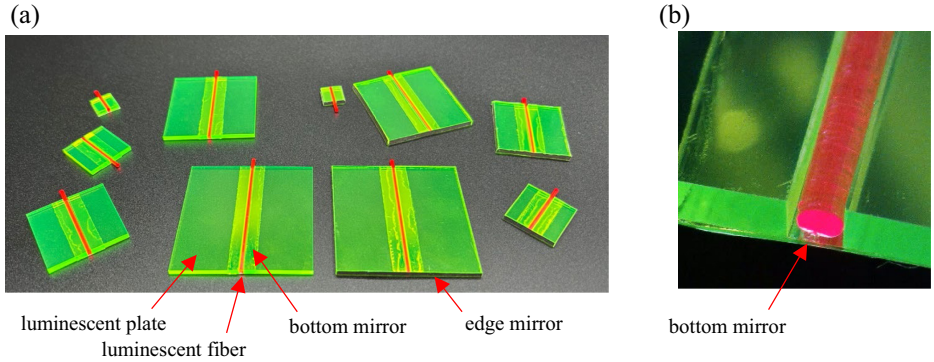

Fig. 2 Photographs of 2.0 mm-thick square samples. (a) The five samples on the right have reflector films attached to their edge surfaces. (b) A microscope photograph of the edge region before attaching a reflective film.

PL photons are leaking out from these irregularities. In addition, the bottom mirror is reflecting the light from some surrounding objects (probably the ceiling light). Their images are blurred, indicating that the bottom and edge mirrors reflect light diffusively. As will become clear later, this has both positive and negative effects on the optical efficiency of a leaf LSC.

Because the existing luminescent components are used, the optical design of our samples is not optimized yet. For example, a larger fiber would accept more green PL photons from the edge surfaces of the plates. Concentrations of the luminescent material in the fiber should be chosen to balance the absorption of the green PL photons and the self-absorption of the red PL photons. Advanced luminescent materials with minimum overlaps between absorption and emission spectra would certainly enhance collection efficiency.

3.2 Measurement

Absorption and emission spectra of the three luminescent components used in our experiments were determined in our previous study.[7] They are reproduced in Fig. 3(a). The emission spectra are normalized such that their integrals represent their quantum yields.

The setup for the measurement is shown in Fig. 3(b). In our previous experiment, we used a power meter to measure the optical power exiting the luminescent fiber, resulting in an approximate estimation of optical efficiency.[9] In this study, spectral photon fluxes are recorded with a spectrometer to evaluate the optical efficiency accurately. A cosine corrector (Model CC-3, Ocean Insight) is attached to the optical fiber head of a spectrometer (Model FLMS13077, Ocean Optics). It is placed near the fiber tip without index-matching oil. Hence, an air gap exists between them. Although this fact decreases the optical efficiency due to Fresnel reflection, we prioritize the ease of handling in this experiment. A mask with an aperture is placed near the edges of the place to prevent the green PL photons from entering the protruded section of the fiber. The coordinate system is defined with x axis on the fiber and y axis along the edge of the two plates. Each sample is placed on a black cloth.

A single spot on the sample is excited by a 1.0 mm-diameter laser beam at 450 nm and the output of the spectrometer is recorded. The excitation spot is stepped on the luminescent plate with fixed intervals in both directions and this recording is repeated. The spectrum of the incident photons is measured by exposing the cosine corrector to the laser beam directly.

For example, the spectra recorded with the largest samples (side length $L = 50$ mm) with and without edge mirrors are compared in Fig. 4. The coordinates of the excited spots (x, y) and the integration time set for the spectrometer t_{int} are indicated in each plot.

When the spots on the fiber are excited directly ($y = 0$), the PL photons with shorter wavelengths become attenuated at larger x, leading to severe redshifts as shown in Fig. 4(a). This is caused by self-absorption in the fiber. As the excitation spot moves away from the origin, this redshift tends to saturate. In addition to self-absorption, PL photons are scattered by some irregularities in the fiber as shown in Fig. 2(b).

When the spots on the plate at $y = 17$ mm are excited, as shown in Fig. 4(b), the spectral flux in units of counts/s·nm becomes one order of magnitude smaller. Because the green PL photons spread in the plate, the redshift in these spectra becomes less apparent.

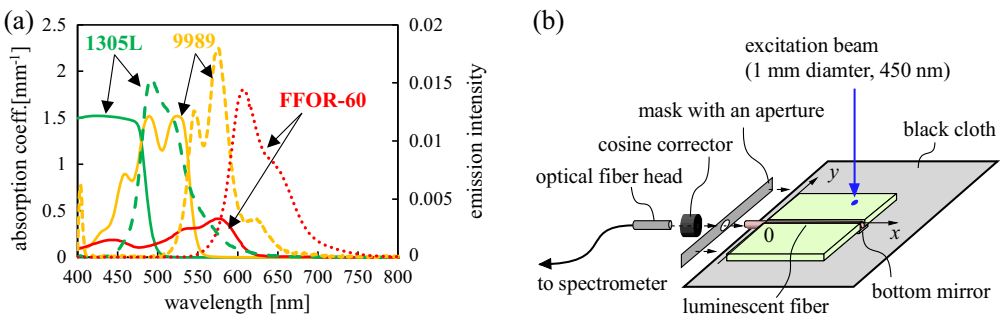

Fig. 3 Single-spot excitation experiment. (a) Absorption coefficients (solid curves) and emission spectra (dotted curves) of three luminescent components.[7] (b) Exploded view of the setup for measuring η_{opt} and definition of the coordinate system.

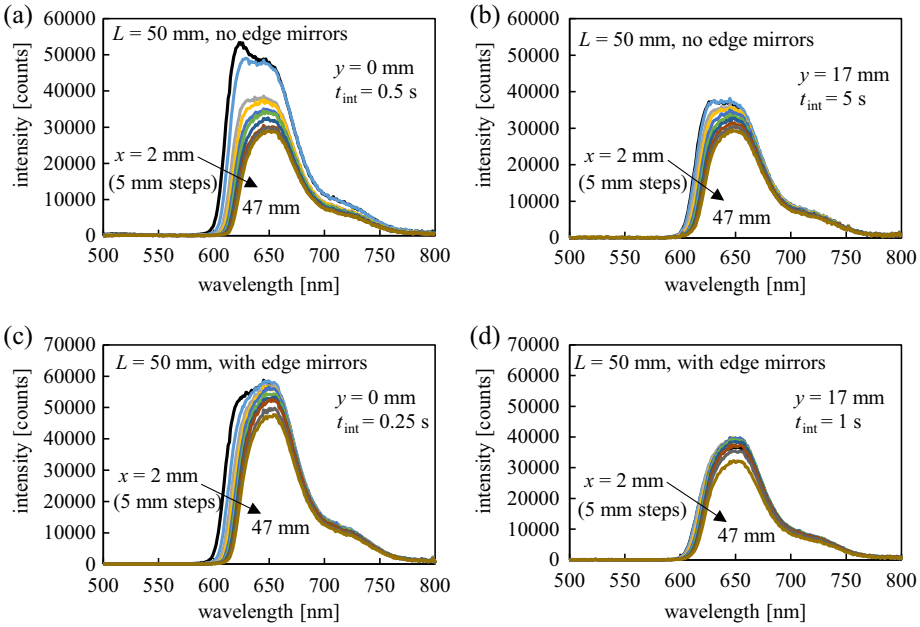

Fig. 4 Spectra recorded with the sample of side length 50 mm. There are no mirrors on its edge surfaces for (a) and (b). Mirrors are attached to its edges for (c) and (d).

As shown in Figs. 4(c) and 4(d), adding mirrors to the edge surfaces increases the spectral fluxes substantially. The redshift is less apparent because the PL photons reflected by the mirrors are added.

3.3 Analysis

The number of the PL photons exiting the fiber per second is proportional to $\int S_{\mathrm{PL}}(\lambda)\mathrm{d}\lambda$ where S_{PL} is the recorded spectrum of the PL photons in units of counts/s·nm. The number of the incident photons is proportional to $\int S_{\mathrm{in}}(\lambda)\mathrm{d}\lambda$ where S_{in} is the recorded spectrum in units of counts/s·nm. Because the same setup is used, the proportionality constants are the same. Hence, the optical efficiency η_{opt} is given by the ratio of these integrals.

Two examples of this analysis are shown in Fig. 5. The optical efficiency in case of the fiber excitation is shown in Figs. 5(a) and 5(b) for the samples with side length $L = 50$ and 20 mm, respectively. The results of the plate excitation are shown in Figs. 5(c) and 5(d) for each sample, respectively. The side length of the sample and the coordinates of the excitation spots are indicated in each plot. The solid and empty markers represent the optical efficiencies of the samples with and without edge mirrors, respectively.

In both cases of the fiber and plate excitation, the optical efficiency of the smaller sample is higher than that of the larger sample. The larger sample exhibits greater dependency on the x coordinate of the excitation spot. These observations are consistent with the PL photon losses during the photon collection process. For example, the PL photons generated in the fiber propagate toward the exiting end and the other end. Those emitted in the wrong direction can be collected after reflection at the other end. However, they are more likely to be lost because they need to traverse longer distances in the fiber. Hence, the collection efficiency decreases as the fiber becomes longer. A similar argument applies to the case of the plate excitation. The PL photons reflected at the edge surfaces are less likely to reach the collecting edge due to the extra distances. Direct excitation of the fiber results in η_{opt} one order of magnitude larger than the plate excitation. Nevertheless, the two strategies (decreasing the side length and attaching mirrors to the edges) enhance η_{opt} substantially.

Note that the optical efficiencies measured here are valid only for excitation at 450 nm. This prompts us to calculate collection efficiency η_{col} by Eq. (2). The absorptance of the luminescent plate was measured to be 0.911 at 450 nm. The average absorptance of the fiber at 450 nm is calculated to be 0.212 for partial exposure of the central 1.0 mm-wide region and 0.181 for full

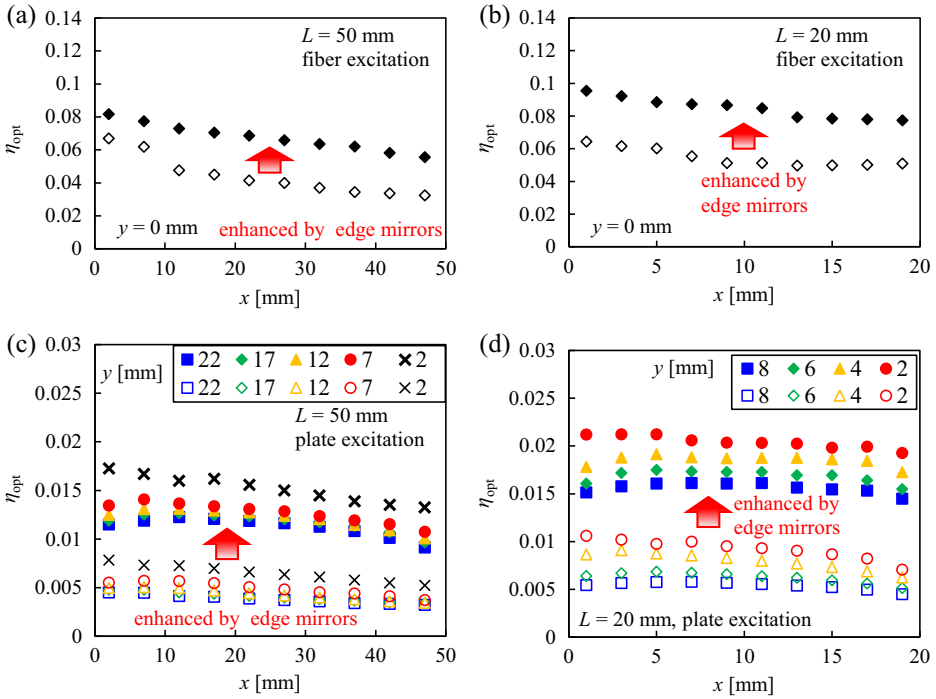

Fig. 5 Position-dependent optical efficiency of two samples. The optical efficiency in case of the fiber excitation for the samples with side length $L = 50$ mm (a) and 20 mm (b). The results of the plate excitation for the sample with $L = 50$ mm (c) and 20 mm (d). Solid and empty markers represent the cases with and without edge mirrors, respectively.

exposure of the whole 1.5 mm-wide region. In this calculation, the transmittance of the luminescent fiber is calculated from Lambert-Beer's law with the absorption coefficients in Fig. 3(a). To account for the reflectance at the fiber-air boundary, a circular fiber cross-section is assumed, and Fresnel equations are used. When a leaf LSC is uniformly irradiated, the collection efficiency is given by averaging the position-dependent collection efficiencies. The results for the cases of the fiber and plate excitation are shown in Figs. 6(a) and 6(b), respectively. Solid and empty markers represent the values with and without the edge mirrors, respectively. Curves are fittings. They will be used for predicting the response of these samples to uniform illumination by a white light source in Sec. 4.1.

Let us regard the $L = 50$ mm sample without edge mirrors as the reference. Its average collection efficiencies are 0.0052 ($\overline{\eta_{\mathrm{col-P}}}$) and 0.21 ($\overline{\eta_{\mathrm{col-F}}}$). Decreasing L from 50 to 10 mm improves these values to 0.0090 and 0.27, respectively. This is 1.7 times increase in $\eta_{\mathrm{col-P}}$ and 1.3 times increase in $\eta_{\mathrm{col-F}}$. Attaching mirrors at the edges of the luminescent components increases $\eta_{\mathrm{col-P}}$ and $\eta_{\mathrm{col-F}}$ to 0.024 and 0.42, respectively. Therefore, the enhancement factor is 4.4 and 2.0 for the plate and the fiber excitation, respectively. Note that the geometric gain

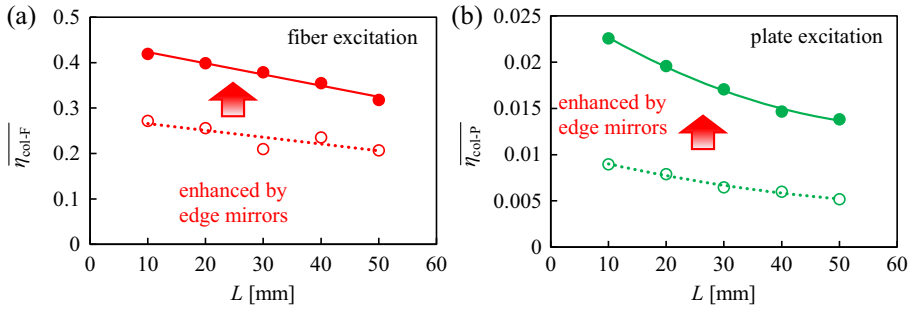

Fig. 6 Average collection efficiency calculated for the case of uniform irradiation. (a) Fiber excitation and (b) plate excitation. The solid and empty markers represent the values for the samples with and without the edge mirrors, respectively. Curves are fittings to be used in Sec. 4.1.

decreases from about 1400 to 57 by decreasing from 50 to 10 mm and that this decrease can be compensated by connecting multiple devices with a clear lightguide.

A theoretical analysis of the trapping efficiency of a PL photon in a luminescent fiber shows that its upper limit is about 0.61 for the fiber with air cladding.[16] The maximum value of $\eta_{\mathrm{col-F}}$ in Fig. 6(a) is 0.47. This discrepancy can be attributed partially to the Fresnel reflection at the air gap between the fiber tip and the cosine corrector and partially to the scattering by the internal and surface irregularities of the fiber used in the experiment.

Regarding the small values of $\eta_{\mathrm{col-P}}$ in Fig. 6(b), the performance of the current samples is limited by the availability of the luminescent components as well as our decision to prioritize the ease of handling. For example, a luminescent fiber with a larger diameter would increase the probability of transferring the green PL photons from the edge of the plates to the fiber. Eliminating the air gap between the fiber tip and the cosine corrector would be effective. The 5 mm-long protruded fiber section should be eliminated for increasing $\eta_{\mathrm{col-P}}$.

4 Uniform Excitation

In this section, we first measure the average optical efficiencies of the 10 samples in Fig. 2(a) by irradiating them uniformly with a white light source. They are compared to the prediction by Eqs. (3) and (5). Agreement will confirm the versatility of the single-spot excitation technique. Next, we show how a tandem structure and underlying surface conditions enhance the photon collection process in leaf LSCs. Finally, the effect of leaf geometry is investigated.

4.1 Measurement

Because white LEDs do not emit in infrared, we can use a Si-based spectrometer to measure their emission spectra. The laser beam in Fig. 3(b) was replaced by a white LED light source. It was placed far away from each sample with edge mirrors to ensure uniform irradiation. A light shield with an aperture surrounded the protruding fiber section so that only the central 1.5 mm-diameter region of the cosine corrector was exposed to the PL photons. This light shield also prevented the protruded fiber section from being exposed to the incident light.

The PL spectra in Fig. 7(a) were acquired when each of the five samples without edge mirrors was irradiated by white LEDs. The dotted curve is the incident spectrum. It was acquired by placing the same module at the irradiated surface and exposing the central 1.5 mm-diameter region of the cosine corrector. The side length L and the integration time set for the spectrometer t_{int} are indicated in each plot. The measurement was repeated with the five samples with edge mirrors. The results are shown in Fig. 7(b).

Optical efficiency is calculated from the PL spectra recorded with these 10 samples. As for the number of incident photons, the recorded incident spectra (the dotted curves in Fig. 7) are multiplied by the areal ratio of each sample and the central 1.5 mm-diameter region of the cosine corrector. The solid and empty markers in Fig. 8 represent the values measured with the samples with and without edge mirrors, respectively. For example, attaching edge mirrors to the largest

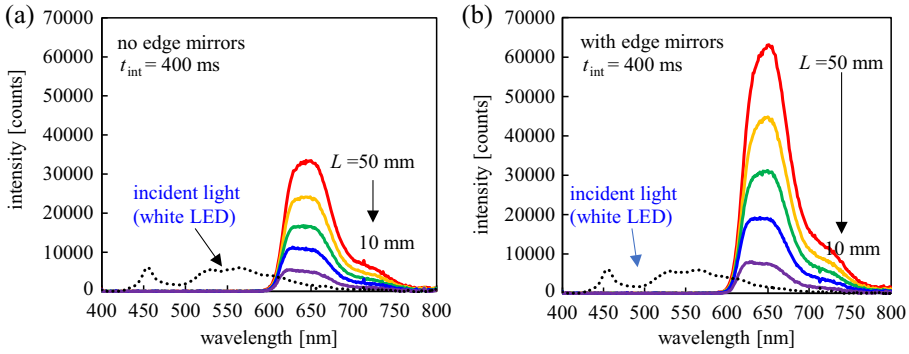

Fig. 7 Spectra recorded with the samples in Fig. 2 under uniform excitation by white LEDs. The spectra in (a) are from the samples without edge mirrors and those in (b) are from the samples with edge mirrors. The solid curves are the spectra of the PL photons from the fiber of each sample. The dotted curve is the spectrum of the excitation light incident on each sample directly.

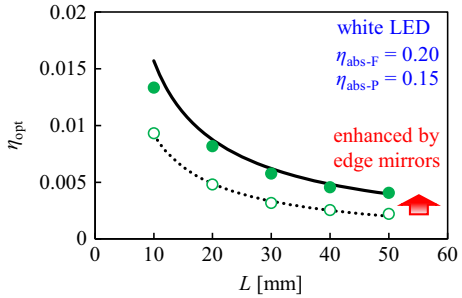

Fig. 8 Optical efficiencies of the 10 samples in Fig. 2 under uniform irradiation by white LEDs. The solid and empty markers are the values measured with the samples with and without edge mirrors, respectively. Curves are the values calculated by Eqs. (3) and (5).

sample ($L = 50$ mm) increases its η_{opt} from 0.0022 to 0.0041. Decreasing L from 50 mm to 10 mm increases η_{opt} from 0.0041 to 0.013 for the sample with edge mirrors.

The solid and dotted curves in Fig. 8 are the average optical efficiencies calculated from the results of the single-spot excitation measurement. Namely, the fitting equations in Fig. 6 were used for the terms η_{col-F} and η_{col-P} in Eq. (5). The term η_{abs-P} was given by Eq. (3). As for the term η_{abs-F}, the distance d in Eq. (3) was varied, and the absorptance was averaged. These values are as indicated in the plot. As shown in Fig. 8, the measured values are reproduced by these curves reasonably well.

The single-spot excitation technique gives more versatile results in the sense that the optical efficiency for the case of non-uniform irradiation by a light source with an arbitrary spectrum can be calculated. However, it takes time to step the excitation spot over the whole incident area of a sample. For this reason, we irradiate various samples uniformly in the following experiments. Nevertheless, the results are only valid for the specific light source used in the measurement.

4.2 Tandem Leaf LSCs

Stacking one LSC on top of another is a well-known approach for enhancing photon collection.[17] We apply this for leaf LSCs. To assemble a lower sample, we used 2.0 mm-thick luminescent acrylic plates emitting in orange (Model 9989, Kanase Inc., Japan). Its quantum yield was measured to be about 77% of the green plate (Model 1305L). The absorption and emission characteristics of this component are shown in Fig. 3(a). A photograph of the sample with side length $L = 50$ mm and a schematic drawing of its cross-section are shown in the inset of Fig. 9(b).

The optical efficiency of this square sample was measured under uniform irradiation by white LEDs. The spectra of the PL photons and the incident light are shown in Fig. 9(a). The curve marked as "tandem" is the sum of the spectra from the upper and lower layers.

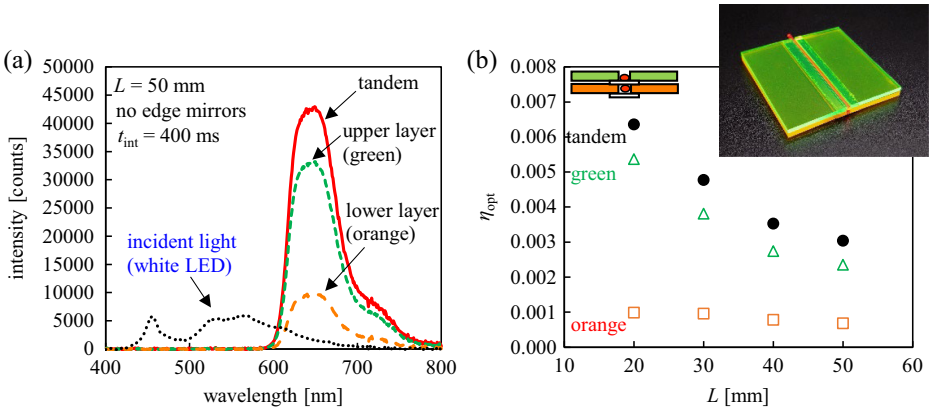

Fig. 9 Optical efficiency measurement with tandem leaf LSCs. (a) Output spectra of a square tandem LSC with side length $L = 50$ mm without edge mirrors under uniform irradiation by white LEDs. (b) The effect of the side length on the optical efficiency.

Samples with different side lengths were assembled and this measurement was repeated. They all had a 10 mm-wide bottom mirror. The result is summarized in Fig. 9(b). For example, in the case of the sample with $L = 50$ mm, its upper layer contributes 78% to the total output. The lower layer contributes 22% by converting the transmitted light and the PL photons emitted downward by the upper layer. Hence, the enhancement factor for adding the orange device is 1.28. The contribution from the lower layer decreases to 16% for the sample with $L = 20$ mm. This is because the bottom mirror of the upper layer blocks the downward photon flux. This effect is more severe for devices with shorter side lengths.

4.3 Underlying Surfaces

It is also well known that a reflective surface below an LSC increases its optical efficiency by reflecting the transmitting incident photons. We have avoided this double passing of the excitation light in our measurement so far by placing our samples on a black cloth.

Here, we study how effective an underlying surface is for a leaf LSC. As described in Sec. 3, the bottom mirror in our sample reflects the transmitted excitation light diffusively. Because this complicates the interpretation of the measurement, we have eliminated the bottom mirror in this experiment. The optical adhesive film used for bridging the two plates comes with a thin supporting transparent film. This film is left unremoved in each sample shown in Fig. 10(a). The PL photons generated by the room light enter this supporting film and escape from its edges. Hence, two bright lines are visible near the fiber in these photographs. They are 10 mm apart. No mirrors are attached to the outer edges.

First, each of the samples was placed on the black cloth and irradiated by the white LEDs. The results are shown by the empty squares in Fig. 10(b). For example, the optical efficiency of the sample with $L = 10$ mm is 0.0061.

Second, a mirror replaced the black cloth. The empty triangles in Fig 10(b) are the results. For example, the optical efficiency of the sample with $L = 10$ mm increases to 0.0084. When the reflected light enters the sample, its optical efficiency becomes 1.38 times larger.

Third, a diffuser film and a mirror were stacked, and each sample was placed on it with an air gap. The results are shown by the empty diamond markers in Fig. 10(b). For example, the optical efficiency of the sample $L = 10$ mm is 0.012. The diffuser/mirror configuration is more effective than the simple mirror because the reflected light enters the sample obliquely and it is more likely to be absorbed.

4.4 Leaf Geometry

The geometry effect of a conventional planar LSC has been studied analytically[18,19] and by ray tracing.[20] We assembled leaf LSCs with various shapes by using the same 2.0 mm-thick luminescent plates and the 1.5 mm-diameter luminescent fiber. Photographs of the samples without edge mirrors are shown in Fig. 11(a). They all have the same incident area of 2500 mm^2, 10-mm-wide bottom mirrors, and a 5-mm-long protruded fiber section. The square sample with a side length of 50 mm serves as a reference. Samples with edge mirrors were also prepared. Each of them was placed on a black cloth and the white LED light source irradiated it uniformly. The PL

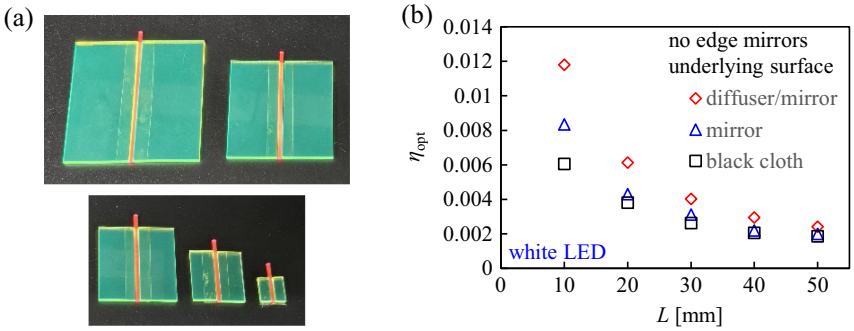

Fig. 10 Square samples without edge mirrors and their optical efficiencies evaluated under uniform irradiation by white LEDs. (a) Photographs of the square samples without bottom mirrors placed on a black cloth. (b) The effects of the underlying surfaces and the side length.

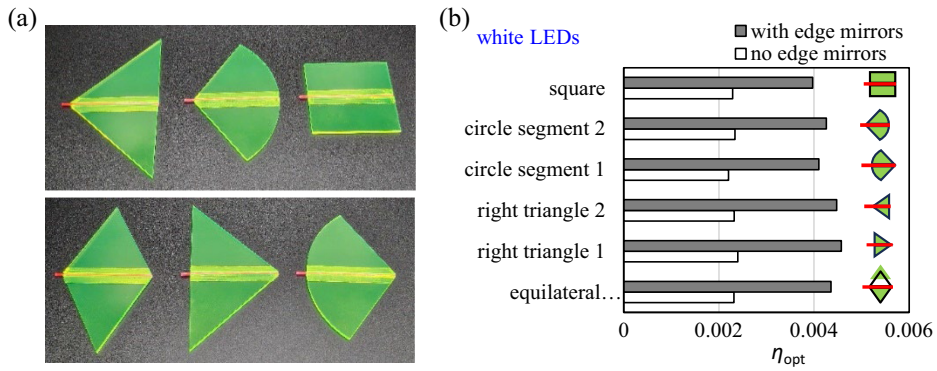

Fig. 11 Leaf LSCs with various shapes. (a) The photographs of the samples without edge mirrors. (b) Optical efficiency evaluated under uniform irradiation by white LEDs.

photons exiting the fiber tip from the side of the protruding section were recorded by the spectrometer. The optical efficiency for each case is compared in Fig. 11(b).

For all the shapes tested in this experiment, η_{opt} is almost doubled by attaching mirrors to the edge surfaces. The sample labeled as "circle segment 1" has the lowest value of 0.0022 among the samples without edge mirrors whereas "right triangle 1" has the highest value of 0.0024. Attaching mirrors to the plate edges increases these to 0.0041 and 0.0046, respectively. Because η_{opt} is weakly dependent on the shape of the luminescent plate, a wide degree of freedom exists in designing the shape of leaf LSCs.

4.5 Maple Leaf LSC

We assembled a sample mimicking a Japanese maple leaf. Four pieces of luminescent plates were cut out of the same 2.0 mm-thick plate by laser cutting. The drawing in Fig. 12(a) shows the three lines for this separation. Although we attempted to polish the edge surfaces after laser cutting, this was not very successful. As shown in Fig. 12(b), the edge surface scatters room light. The same adhesive optical films were used to bridge them with gaps in between. These transparent supporting films were left unremoved. The luminescent fibers were inserted to these gaps, and they sat on the adhesive side of the supporting films. The total incident area of this sample is 954 mm^2.

The photographs in Fig. 12(c) show the sample placed on three different surfaces. When it is either on a black cloth or a mirror, the edges of the supporting films are visible. The underlying surface changes the appearance of the sample. It looks yellowish when it is on a diffuser film stacked on a mirror. Room light is reflected diffusively and added to the green PL photons emitted by the sample.

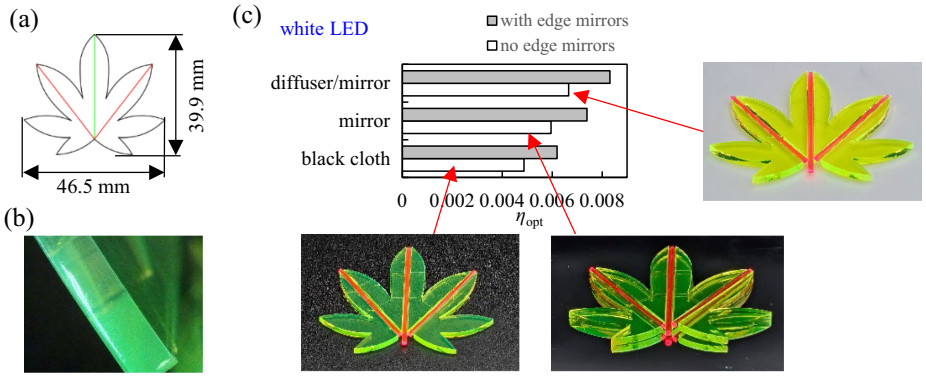

Fig. 12 Maple leaf LSC. (a) A drawing illustrating the three lines for laser cutting. (b) A photograph of the edge of the 2.0 mm-thick luminescent plate after laser cutting and our polishing attempt. (c) Optical efficiency evaluated under uniform irradiation by white LEDs and photographs of the sample without edge mirrors.

Under the illumination by the white LEDs, the PL photons exiting the three fibers were recorded by the spectrometer. The output of the sample was calculated by adding and integrating these spectra. The number of incident photons was measured as before. Optical efficiency η_{opt} was evaluated for each underlying surface. After the edge mirrors were attached, the measurement was repeated.

The plot in Fig. 12(c) summarizes the results. The smallest η_{opt} value is 0.0049. As shown in Fig. 8(a), the square sample of $L = 20$ mm has η_{opt} of 0.0048 under the same conditions (no edge mirrors, black cloth, white LEDs). This is reasonable because the PL photons in the maple leaf configuration propagate shorter distances in the plates and longer distances in the fiber. Attaching edge mirrors increases η_{opt} to 0.0062. This enhancement by edge mirrors is noticeably smaller than the cases in Figs. 8(a) and 11(b). This is likely caused by our lack of polishing skill. As shown in Fig. 12(b), the edge surface does not look clear. Regarding the effect of the underlying surface condition, a similar trend is observed in Figs. 12(c) and 11(b). Thus, a diffusive mirror has a negative effect if used as an edge mirror and a positive effect if used as an underlying layer.

5 Conclusions

A large-scale LSC suffers from photon losses during waveguiding. A leaf LSC offers a solution to this problem. It is configured by placing luminescent plates in the vicinity of a luminescent fiber with their edge surfaces facing the fiber. By connecting multiple fibers to a clear lightguide and attaching a PV cell to its end, one can enlarge the total incident area without increasing the propagation distance of the PL photons. Although connecting N devices leads to a roughly N-fold increase in photocurrent without sacrificing geometric gain, it is still desired to enhance photon collection in a single device. Some techniques reported for conventional planar LSCs have been applied to leaf LSCs.

In theory, the optical efficiency of a leaf LSC is expressed in terms of collection efficiency and absorptance of each luminescent component. Once these parameters are determined by experiment and/or ray tracing simulations, the optical efficiency of a leaf LSC under an arbitrary spectral photon flux can be calculated. Hence, one can predict the performance of a leaf LSC in a real-world application.

In the experiment, we assembled leaf LSCs with off-the-shelf luminescent components. Their optical efficiency was evaluated by exciting a single spot on each component with a small laser beam and recording the spectral flux exiting the fiber. The redshift in the PL spectrum becomes more apparent due to self-absorption as the excitation spot on the plate moves away from the fiber. Position-dependent collection efficiency was obtained from the optical efficiency measured for each excitation spot and the spectral absorptance of each component. For example, the average efficiency of collecting PL photons generated in the plate of 2.0 mm-thick square leaf LSCs increased from 0.0052 to 0.024 by decreasing its side length from 50 to 10 mm and attaching edge mirrors. In the case of fiber excitation, the average collection efficiency increased from 0.21 to 0.42 by these measures. We also irradiated our samples uniformly with a white LED light source. The sample with a side length of 50 mm and without edge mirrors exhibited the smallest value of 0.0022. The highest optical efficiency of 0.013 was obtained by decreasing the side length to 10 mm and attaching mirrors to the edge surfaces. These values are consistent with those predicted by the model.

The photon collection process in a leaf LSC was enhanced by decreasing its lateral size and attaching mirrors to the outer edges of its luminescent components. Other familiar techniques such as tandem structures and underlying reflective surfaces were effective to varying degrees. For example, placing an orange device beneath a green one increased the optical efficiency of our 2.0 mm-thick square sample with a side length of 50 mm by 28% in case of uniform irradiation by white LEDs. A diffusive reflector underneath a leaf LSC was more effective. The optical efficiency of our sample with a side length of 10 mm was almost doubled by a diffusive reflector under the irradiation by the white LEDs. Note that these numbers are valid only for the specific light source used in the measurement. On the other hand, the optical efficiency of a leaf LSC is weakly dependent on the leaf geometry. This fact extends the degree of freedom for designing leaf shapes. Nevertheless, the current experiment is limited by the available luminescent components. Further efficiency enhancement is expected by adopting advanced luminescent

materials, optimizing their concentrations, and improving the optical design of the leaf-like structure, such as the optical coupling between the plates and the fiber.

Disclosures

The authors declare no conflicts of interest.

Code and Data Availability

Data underlying the results presented in this paper are not publicly available at this time but may be obtained from the authors upon reasonable request.

Acknowledgments

We thank Yu Kawano for his advice on characterizing the luminescent plates. Our gratitude is extended to Tadamasa Anekawa and other members of our laboratory for their assistance in the experiments and Toru Maruyama at the machine shop for his assistance in laser cutting.

References

1. W. H. Weber and John Lambe, "Luminescent greenhouse collector for solar radiation," *Appl. Opt.* **15**(10), 2299–2300 (1976).
2. I. Papakonstantinou, M. Portnoi, and M. G. Debije, "The hidden potential of luminescent solar concentrators," *Adv. Energy Mater.* **11**, 2002883 (2021).
3. B. S. Richards and I. A. Howard, "Luminescent solar concentrators for building integrated photovoltaics: opportunities and challenges," *Energy Environ. Sci.* **16**, 3214–3239 (2023).
4. J. S. Batchelder, A. H. Zewai, and T. Cole, "Luminescent solar concentrators. 1: Theory of operation and techniques for performance evaluation," *Appl. Opt.* **18**(18), 3090–3110 (1979).
5. R. Mazzaro and A. Vomiero, "The renaissance of luminescent solar concentrators: the role of inorganic nanomaterials," *Adv. Energy Mater.* **8**, 180190 (2018).
6. M. Cao, X. Zhao, and X. Gong, "Achieving high-efficiency large-area luminescent solar concentrators," *JACS Au* **3**, 25–35 (2023).
7. H. Nishimura et al., "Leaf-inspired luminescent solar concentrator based on two-stage photoconversion," *Opt. Express* **31**(14), 22444–22456 (2023).
8. T. Liu, J. Chen, and K. Huang, "Highly efficient Y-junctions with arc-bend branch structures of sunlight guiding systems for indoor illumination," *J. Chin. Inst. Eng.* **41**(5), 387–394 (2018).
9. H. Nishimura et al., "Design considerations for leaf-inspired luminescent solar concentrators based on two-stage photoconversion," *Proc. SPIE* **12671**, 126710F (2023).
10. J. C. Goldschmidt et al., "Increasing the efficiency of fluorescent concentrator systems," *Sol. Energy Mater. Sol. Cells* **93**(2), 176–182 (2009).
11. C. Yang, et al., "Consensus statement: standardized reporting of power-producing luminescent solar concentrator performance," *Joule* **6**(1), 8–15 (2022).
12. I. Fujieda and Y. Tsutsumi, "Extending the concept of edge collection function to polygonal and curved planar luminescent waveguides," *J. Photonics Energy* **10**(4), 044501 (2020).
13. O. Y. Edelenbosch et al., "Luminescent solar concentrators with fiber geometry," *Opt. Express* **21**, A503–A514 (2013).
14. I. Parola et al., "High performance fluorescent fiber solar concentrators employing double-doped polymer optical fibers," *Sol. Energy Mater. Sol.* **178**, 20–28 (2018).
15. G. Keil, "Radiance amplification by a fluorescence radiation converter," *J. Appl. Phys.* **40**, 3544–3547 (1969).
16. J. D. Weiss, "Trapping efficiency of fluorescent optical fibers," *Opt. Eng.* **54**(2), 27101 (2015).
17. A. Goetzberger and W. Greubel, "Solar energy conversion with fluorescent collectors," *Appl. Phys.* **14**, 123–139 (1977).
18. E. Loh and D. J. Scalapino, "Luminescent solar concentrators: effects of shape on efficiency," *Appl. Opt.* **25**, 1901–1907 (1986).
19. I. Sychugov, "Geometry effects on luminescence solar concentrator efficiency: analytical treatment," *Appl. Opt.* **59**, 5715–5722 (2020)
20. X. Zhu, M. G. Debije, and A. H. M. E. Reinders, "Simulation of the effects of geometry on performance of luminescent solar concentrator photovoltaic devices," *IEEE J. Photovoltaics* **14**(1), 116–122 (2024).

Hiroto Nishimura received his BS and MS degrees from Ritsumeikan University in March 2022 and March 2024, respectively. He is currently with Central Japan Railway Company. He co-authored a paper on luminous reflective displays.

Kohei Okada received his BS and MS degrees from Ritsumeikan University in March 2022 and March 2024, respectively. He is currently with Shimadzu Corporation.

Atsuya Suzuki received his BS and MS degrees from Ritsumeikan University in March 2022 and March 2024, respectively. He is currently with Toyota Boshoku Corporation.

Yuta Mizuno received his BS and MS degrees from Ritsumeikan University in March 2022 and March 2024, respectively. He is currently with Sharp Corporation.

Ichiro Fujieda is a professor at Ritsumeikan University. He received his PhD from the University of California, Berkeley, in 1990. He was with Xerox Palo Alto Research Center (1990 to 1992) and NEC Corporation (1992 to 2003) before joining Ritsumeikan University in 2003.